samples at 1.06 μ indicate that the lowest absorption coefficient for currently available bulk material is ~ 0.7 cm^{-1}, which makes these crystals unsuitable for Raman oscillator applications with the Nd-YAG laser.

The method described here is well suited to measure-ments of r_{ijk} on wurtzite or zinc-blende-type crystals with conductivity too large to sustain low-frequency modulating fields. It also provides more accurate mea-surements of ξ_{ijk} than present high-power-pulsed SHG measurements.

Measurement of the Lowest-Order Nonlinear Susceptibility in III–V Semiconductors by Second-Harmonic Generation with a CO₂ Laser*

J. J. WYNNE† AND N. BLOEMBERGEN

Gordon McKay Laboratory, Harvard University, Cambridge, Massachusetts 02138

(Received 8 July 1969)

Both the magnitude and sign of the nonlinear susceptibility $d_{14}{}^{NL}(-2\omega,\omega,\omega)$ describing second-harmonic generation at 10.6 μ have been measured in wedge-shaped semiconducting samples using a Q-switched CO₂ laser. The results are (in units of 10^{-6} esu): d_{14}= +1.0 for InAs, +0.45 for GaAs, +0.26 for GaP, and +1.5 for GaSb. The limits of error are discussed, and the results are compared with previous experimental data and with several recent theoretical calculations. The effect of uniaxial compression on the coherence length for second-harmonic generation is also measured.

I. INTRODUCTION

THE nonlinear susceptibility describing second-harmonic generation in III-V and II-VI semiconductors was first measured in the visible and near-infrared region of the spectrum. Patel[1,2] first observed the second-harmonic generation (SHG) in these materials with a CO₂ laser beam. He pointed out the difficulties in obtaining accurate values for the non-linearity which are associated with the long coherence length. He measured the transmission through a plane-parallel slab which could be rotated. This technique, first introduced by Maker et al.,[3] presents difficulties in high-index materials with long coherence lengths. It is difficult to control the geometry, and because of the high Fresnel reflection coefficient, significant changes in the fundamental intensity distribution are caused by the standing-wave pattern inside the plane-parallel slab. In addition, the absorption in samples which are many coherence lengths thick may be sig-nificant. The experimental corrections are large and uncertain. It should be pointed out that the observation of second harmonic (SH) in reflection obtained in the visible region is free from these uncertainties.[4] It is of considerable interest to obtain reliable values of the

nonlinear susceptibility in the far infrared, because these values may be compared more readily with theoretical calculations. These make use of the low-frequency approximation, in which all energy denomi-nators are replaced by an effective energy-band gap. Several of such calculations have recently been pub-lished for the simple structures of III-V and II-VI semiconductors. The experiments to be described in this paper were, in fact, a stimulus for these calculations. The results of the next-higher-order nonlinearity, de-scribing third-order optical mixing, have already been published.[5]

The experimental method of determining both the magnitude and the sign of the susceptibility for SHG in these high-index materials is described in Sec. II. The determination of the sign is new and the results for the magnitude, believed to be more accurate, are compared with previous experimental results and with theoretical calculations in Sec. III. In a final section the effect of uniaxial compression on the coherence length is investigated. It was originally hoped that phase matching in these materials could be achieved in this manner, but the required uniaxial stresses are too large.

II. EXPERIMENTAL METHOD

The experimental difficulties associated with SHG in transmission through a plane-parallel plate of high-index material with small dispersion, mentioned in the Introduction, are discussed in more detail in Appendix A2 of the Ph.D. thesis of one of the authors (J.J.W.).[6]

[1] C. K. N. Patel, Phys. Rev. Letters **15**, 1027 (1965).

[2] C. K. N. Patel, Phys. Letters **16**, 613 (1966).

[3] P. D. Maker, R. W. Terhune, M. Nisenoff, and C. M. Savage, Phys. Rev. Letters **8**, 21 (1962).

[4] N. Bloembergen, R. K. Chang, J. Ducuing, and P. Lallemand, in *Proceedings of the Seventh International Conference on the Physics of Semiconductors* (Dunod Cie., Paris, 1964), p. 121.

[5] J. J. Wynne, Phys. Rev. **178**, 1295 (1969).

[6] J. J. Wynne, Ph.D. thesis, Harvard University, 1969 (un-published).

These difficulties can be eliminated by the use of wedge-shaped samples. The crystals to be measured are ground and polished to a wedge with an apex angle of roughly 2°–3°. The thickness at the base of the prism is about five to ten times the coherence length l_{coh}.

The experimental arrangement, which also allows the determination of the relative sign of the non-linearity, is shown in Fig. 1. A beam of finite aperture enters the sample, generates SH, and is multiply reflected and transmitted. The wedged shape causes each successive transmitted beam to travel in a different direction. A focusing lens and detector can be positioned to collect only the initial transmitted beam and the SH it generates. Then all the problems of multiple reflection interference are avoided. By displacing the wedge as indicated in the Fig. 1, the light path length through the sample may be varied and l_{coh} determined. A wedge no more than five or six l_{coh} thick at the thick end allows accurate measurements of l_{coh}. Because a thin sample may be used, absorbing crystals with $\alpha \sim 10$ cm^{-1} at both fundamental and SH may be measured in transmission. Using this technique, we have measured the nonlinear susceptibility in the materials GaAs, InAs, GaP, and GaSb. The last of these is absorbing ($\alpha > 3$ cm^{-1}) due to free-carrier absorption even in the purest samples available.

The relative sign of two samples may be determined from the interference of the SH generated by the same laser beam passing through two consecutive wedges. The sapphire plate absorbs 10.6 μ and transmits 5.3 μ. With the sapphire in place, SH is generated only in the first wedge. No fundamental reaches the second wedge, so it acts only as a linear dielectric which refracts the SH generated in the first wedge into the detector. By displacing the wedge, as shown, its coherence length can be measured. With the sapphire removed, both fundamental and SH enter wedge b, where more SH is generated. The resultant enters the detector which has a separate sapphire filter to remove the transmitted fundamental. By studying the intensity of total SH as each wedge is displaced, the relative signs of the non-linear susceptibility may be determined. Note that for the materials studied, both 10.6 and 5.3 μ are far from absorption edges, so that the susceptibilities are real.

The geometry of Fig. 1 is also used to measure the relative magnitude of susceptibilities. With the sapphire
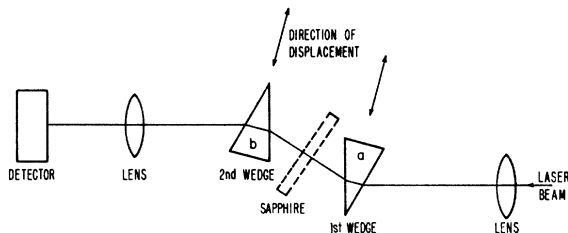

FIG. 1. Schematic experimental arrangement. The removable sapphire slab absorbs the fundamental laser beam at 10.6 μ but passes the second harmonic at 5.3 μ.

in place only wedge a is being measured. By replacing wedge a with another material and seeing how the SH changes, accurate relative values for the absolute value of the nonlinear susceptibilities of the two materials may be determined.

The Q-switched CO$_2$ laser was similar in construction to that described by Patel.[2] The outputs of several P-branch transitions were isolated by the use of a narrow-band interference filter. Typical output power ranged from 0.5 to 5 kW in a pulse about 2×10^{-7} sec long. The pulse repetition rate was 200 cps. The output was linearly polarized by the NaCl brewster angle windows on the 6-ft-long discharge tube with a 1-in. inner diameter. Transverse-mode control was achieved by the size of an iris diaphragm. The intensity distribution through the partially transmitting output mirror was a nearly diffraction-limited Gaussian beam.

The SH near 5.3 μ was detected by a Au-doped germanium photoconductive detector manufactured by Santa Barbara Research Corp. The detector was mounted on a cold finger in a liquid-nitrogen filled Dewar with a BaF$_2$ window. The output pulses were fed into a boxcar integrator (Princeton Applied Research model CW-1). Further details of the experimental equipment and procedures may be found in Ref. 6.

A. Determination of Relative Magnitude of Nonlinear Susceptibility

The laser field is polarized parallel to the [111] crystallographic direction of the crystal, which is also parallel to the edge of the wedged sample, as shown in Fig. 2. Under these conditions the nonlinear polarization is also parallel to this direction and has the magnitude

$$P_0^{NL}(2\omega) = [2/(3)^{1/2}]d_{14}E^2(\omega). \tag{1}$$

The real amplitude of the laser field inside the crystal is denoted by $E(\omega)$, and $d_{14} = X_{xyz}^{NL}(-2\omega, \omega, \omega) = X_{xzy} = X_{yzx} = X_{yxz} = X_{zyx} = X_{zxy}$. With these conventions the value of d_{14} is one-half of the constants listed by Robinson.[7]

If the reflected harmonic wave is ignored, the second-harmonic field generated by a traveling fundamental wave at a distance z from the plane of entry is

$$E(2\omega) = \frac{4\pi i \omega}{n_2 c} P_0^{NLS} \frac{e^{-i\Delta k z + \Delta \alpha z/2} - 1}{-i\Delta k + \frac{1}{2}\Delta \alpha}. \tag{2}$$

Here n_2 is index of refraction at 2ω, $\Delta k = k(2\omega) - 2k(\omega)$ is momentum mismatch, and $\frac{1}{2}\Delta \alpha = \frac{1}{2}\alpha(2\omega) - \alpha(\omega)$ is the difference of the amplitude attenuation coefficient at 2ω minus the power absorption coefficient at ω.

For negligible absorption the SH intensity, from Eqs. (1) and (2), is given by

$$|E(2\omega)|^2 = \frac{64\omega^2 l_{coh}^2}{n_2^2 c^2} \sin^2\left(\frac{\pi z}{2l_{coh}}\right)\frac{4}{3}d_{14}^2|E(\omega)|^4, \tag{3}$$

[7] F. N. H. Robinson, Bell System Tech. J. 46, 913 (1967).

TABLE I. Experimental values of d_{14} in III-V semiconductors, relative to d_{14}(InAs).

	InAs	GaAs	GaP	GaSb
l_{coh}(meas) (μ)	53±2	104±7	46±3	134±7
l_{coh}(calc) (μ)	63[a]	...	63[b]	
$T(2\omega)/T(2\omega)$ (InAs)	1	(1.09±15)%	(0.092±15)%	(10.0±15)%
$n(\omega)$[c]	3.49	3.27	3.05	3.80
$R(\omega)$	0.308	0.283	0.256	0.340
$n(2\omega)$[c]	3.54	3.30	3.11	3.82
$R(2\omega)$	0.314	0.286	0.263	0.342
d_{14}/d_{14}(InAs)	1	(+0.45±10)%	(+0.26±10)%	(+1.51±10)%

[a] From index-of-refraction data of O. G. Lorimor and W. G. Spitzer, J. Appl. Phys. **36**, 1841 (1965).
[b] From index-of-refraction data of D. A. Kleinman and W. G. Spitzer, Phys. Rev. **118**, 110 (1960).
[c] From transmission measurements of samples coupled with measured $l_{coh} = \lambda_0/4[n(2\omega) - n(\omega)]$.

where the coherence length $l_{coh} = \pi/\Delta k$ has been introduced. With the laser operating in the fundamental transverse Gaussian mode, the cross section of the field amplitude distribution $E(\omega)$ is given, in the near-field approximation, by

$$E(\omega) = B(\omega)e^{-r^2/w_1^2}e^{ikz}, \quad (4)$$

where w_1 is the beam-spot size.[8] The total power may be obtained by integrating over the cross-sectional area. The total time-averaged power at the fundamental is

$$T(\omega) = \tfrac{1}{16}n(\omega)cw_1^2 |B(\omega)|^2. \quad (5)$$

The SH spot size is $w_2 = w_1/(2)^{1/2}$ and SH total line-averaged power is

$$T(2\omega) = \frac{T^2(\omega)512\omega^2\tfrac{4}{3}d_{14}^2(l_{coh})^2}{(n_1)^2 n_2 c^3 (w_1)^2}\sin^2\left(\frac{\pi z}{2l_{coh}}\right), \quad (6)$$

where $n_1 = n(\omega)$. This expression gives the well-known maxima and minima of the Maker experiment. The maxima occur if z is an odd integral number of coherence lengths, while zero intensity occurs for an even number of coherence lengths.

The path length z was changed by moving the wedge transverse to the beam. With the focused spot diameter of $\sim$500 μ, and with wedge angles of $\sim$0.04 rad, the crystal thickness varies by 20 μ across the focused beam. With $l_{coh} = 50$ μ, the factor $\sin^2(\pi z/2l_{coh})$ is partially averaged over this cross section. When the center of the spot traverses exactly an odd number of l_{coh}, the edge of the beam would create a SH power proportional to $\sin^2[\tfrac{1}{2}\pi(0.08)]\cong0.9$. So the error introduced by the beam spread is not very great. Only a small fraction of the beam will be traversing a length of crystal significantly different from that traversed by the center of the beam. However, when setting the wedge to get zeros of SHG, a true zero will be impossible because of the beam width. This showed up most clearly for the case of GaP, which had the shortest coherence length of the crystals studied.

[8] G. D. Boyd and J. P. Gordon, Bell System Tech. J. **40**, 489 (1961).

In determining relative magnitudes of d_{14} the geometry of Fig. 1 was used. With the sapphire in place, wedge b plays a passive role. Wedge a was alternatively InAs and another crystal, each with the same crystallographic orientation. Each crystal was set to maximize the SH power. Since laser power, spot size, and mode structure are constant from one crystal to the next, a comparison of external SH power from material A and material B produces the following according to Eq. (6):

$$\left(\frac{T_B(2\omega)}{T_A(2\omega)}\right)_{ext} = \left[\frac{d_{14}(B)}{d_{14}(A)}\right]^2\left[\frac{(l_B)_{coh}}{(l_A)_{coh}}\right]^2\left[\frac{(n_1)_A{}^2(n_2)_A}{(n_1)_B{}^2(n_2)_B}\right]$$
$$\times\frac{[1-R_B(\omega)]^2[1-R_B(2\omega)]}{[1-R_A(\omega)]^2[1-R_A(2\omega)]}. \quad (7)$$

$R = (n-1)^2/(n+1)^2$ is the linear Fresnel power reflection coefficient. The reflectivity changes with the sample, so that the laser power transmitted by the entrance face is $[1-R(\omega)]T(\omega)_{ext}$. The SH power
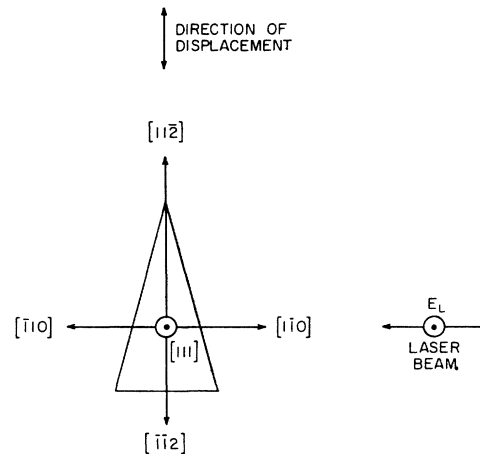
FIG. 2. Geometry of the light beams, polarization and crystallographic orientation.
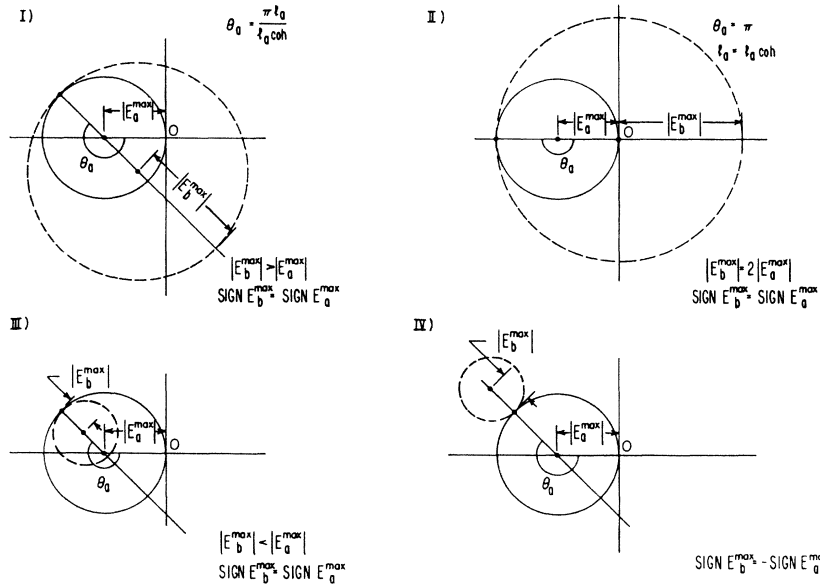
FIG. 3. Interference of SH waves generated in two nonabsorbing slabs, traversed by the same beam. The resultant amplitude, as the length of the b sample is varied, is given by the distance from the origin O to a point on the dotted circle.

transmitted by the back face is

$$T(2\omega)_{\text{ext}} = [1 - R(2\omega)]T(2\omega)_{\text{int}}.$$

The data resulting from relative measurements of SH power and coherence length are presented in Table I along with the values of the indices of refraction and the reflectivities used to calculate the values of d_{14} from Eq. (7), relative to InAs. The uncertainty in this relative value of d_{14} is a result of the uncertainty in the relative power measurements, the uncertainty in the l_{coh} measurements, and a small uncertainty in the index-of-refraction values. The indices were all measured with samples cut from the same bulk samples which were the sources for the wedges.

The maximum thickness of the GaSb wedges was 500 μ. In the samples of GaSb the power absorption coefficients were determined from the linear transmission measurements. At the SH and fundamental they were $\alpha_2 = 3.6$ cm^{-1} and $\alpha_1 = 7.8$ cm^{-1}, respectively. In the notation of Eq. (2), $\Delta\alpha = \alpha_2 - 2\alpha_1 = -12$ cm^{-1}. Since $\Delta k(\text{GaSb}) = \pi/l_{\text{coh}} = 225$ cm^{-1}, we can see from Eq. (2) that the positions of the maxima and minima as a function of z for $z \leq 0.5$ mm are not changed significantly from the case without absorption. This ensures that the measurement of l_{coh} was accurate despite absorption since thin samples were used. In addition, for this thickness the corrections due to absorption are expected to be small enough to be neglected in using the SH power comparison to determine the relative value of $d_{14}(\text{GaSb})$. Experimentally the observed SH power for $l = 3(l_{\text{coh}})$ was equal to that for $l = l_{\text{coh}} = 134$ μ to within the experimental accuracy of the relative power measurement. This ensures that absorption was not affecting our results for these thin samples. Note that for thicker samples, the Δk dependence of $T(2\omega)$ will eventually disappear. This is why thin samples are

necessary to measure d_{14} and l_{coh} in absorbing crystals like GaSb.

B. Sign of d_4

When the sapphire plate in Fig. 1 is removed, SH polarization is created in both wedges. If the path length in the first prism is l_a and in the second l_b and the maximum SH amplitude generated in an odd number of coherence length in each prism alone is $2E_a{}^{\text{max}}$ and $2E_b{}^{\text{max}}$, then the combined SH field amplitude from the two prisms, traversed by the same laser beam, is

$$E_{ab}(2\omega) = E_a{}^{\text{max}}(e^{-i\pi l_a/(l_a)_{\text{coh}}} - 1) + E_b{}^{\text{max}}e^{-i\pi l_a/(l_a)_{\text{coh}}}$$
$$\times (e^{-\pi l_b/(l_b)_{\text{coh}}} - 1). \quad (8)$$

If the two wedges are made of the same material and have the same crystallographic orientation, one obviously has $E_a{}^{\text{max}} = E_b{}^{\text{max}}$ and $(l_a)_{\text{coh}} = (l_b)_{\text{coh}}$. In this case Eq. (8) gives the same result as for a single slab of thickness $l_a + l_b$.

Since the crystals are nonabsorbing in the frequency range of interest, both $E_a{}^{\text{max}}$ and $E_b{}^{\text{max}}$ are real. By observing the SH intensities of each wedge separately, the magnitudes $|E_a{}^{\text{max}}|^2$ and $|E_b{}^{\text{max}}|^2$ are determined. The relative sign of $E_a{}^{\text{max}}$ and $E_b{}^{\text{max}}$ is then determined from the observed intensity of the combination $|E_{ab}|^2$. Some typical phasor diagrams are shown in Fig. 3. For a given choice of l_a, the magnitude $|E_{ab}|$ is given by the distance from the origin to a point on the dotted circle. The circle has a diameter $|2E_b{}^{\text{max}}|$ and is traced out as l_b is varied. Note that there is no variation in the combined intensity if $E_b{}^{\text{max}} = 2E_a{}^{\text{max}}$ and $l_a = l_{a,\text{coh}}$. For $|E_b{}^{\text{max}}| < 2|E_a{}^{\text{max}}|$ and $l_a = l_{a,\text{coh}}$, the combined intensity $|E_{ab}|^2$ will decrease if $E_b{}^{\text{max}}$ and $E_a{}^{\text{max}}$ have the same sign; the combined intensity always increases

if they have opposite sign. This interference method has been used previously.[9]

To determine the relative sign of d_{14} it is necessary to know the absolute orientation of the crystal, i.e., one must distinguish between the [111] and [$\bar{1}\,\bar{1}\,\bar{1}$] crystallographic directions. We take the positive [111] direction pointing from a type-III atom towards a nearest-neighbor type-V atom in the $\bar{4}3m$ crystal structure. A type-A face has the outward pointing normal in this positive [111] direction and has type-III atoms as the atomic layer closest to the surface. A type-B face points in the opposite, [$\bar{1}\,\bar{1}\,\bar{1}$], direction and has type-V atoms closest to the surface. These two directions may be distinguished by chemical etching techniques, which have been related to the absolute atomic configuration by x-ray diffraction near an absorption edge and the sign of the piezoelectric effect.[10] The results of the etching are shown in Table II.

Wedges for GaAs, GaSb, and InSb were prepared and oriented so that their positive [111] in the arrangement of Figs. 1 and 2 were parallel. It was found that the sign of $E_a{}^{\max}$ and $E_b{}^{\max}$ was the same under these conditions. This implies that d_{14} has the same sign for these materials.

Unfortunately, crystals of GaP were not available to make wedges in this orientation. Wedges were cut out of platelets of GaP and InAs with the $\langle 111 \rangle$ direction perpendicular to the broad faces as shown in Fig. 4. After etching had distinguished the A and B faces, an x-ray picture was taken of each sample with the A face facing the incident x-ray beam. Each x-ray picture yielded zone lines which could be identified as $\langle 110 \rangle$ or $\langle 112 \rangle$ directions going through the center of the picture.

TABLE II. Etches used to distinguish A and B faces in the III-V compounds.

Material	Chemical composition	Etch Conditions
InAs	HCl[a]	Almost immediately the B face turns black. The A face develops characteristic etch pits.
GaAs	1 HF[b] 3 HNO₃ 2 H₂O	Etch for 10 min. The A face becomes pitted. The B face does not develop pits.
GaP	Bubble chlorine[c] gas through CH₃OH until it turns green	Etch for 3 min. The A face becomes pitted. The B face is chemically polished.
GaSb	1 Br₂[d] 10 CH₃OH	Etch for 20 sec. The A face becomes pitted. The B face does not develop pits.

[a] This etch is described in H. C. Gatos and M. C. Lavine, MIT Lincoln Laboratory Technical Report No. 293, 1963 (unpublished). It is given as etch No. 23 on p. 39.
[b] Etch No. 12 (Ref. a, p. 39).
[c] Etch suggested by Lars Luther of Bell Telephone Laboratories.
[d] Etch No. 15, (Ref. a, p. 39).

[9] R. K. Chang, J. Ducuing, and N. Bloembergen, Phys. Rev. Letters 15, 6 (1965); H. J. Simon and N. Bloembergen, Phys. Rev. 171, 1104 (1968).
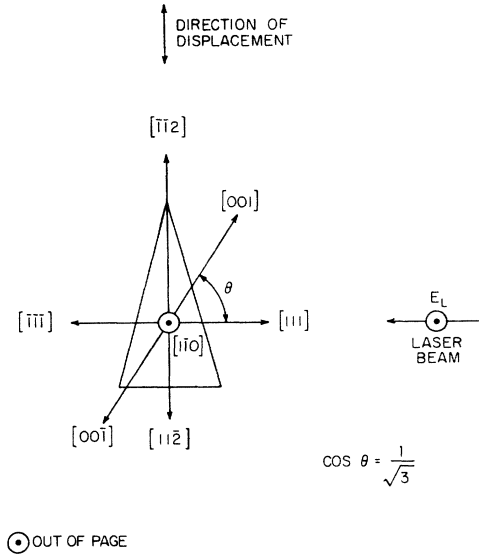[10] H. C. Gatos and M. C. Lavine, J. Electrochem. Soc. 107, 427 (1960), and references cited therein.

FIG. 4. Orientation of the GaP sample.

In addition, the [$\bar{1}$10] direction was distinct from the [1$\bar{1}$0], although we could not tell which was which. But since both InAs and GaP have identical Bragg-reflection planes, they could be rotated around $\langle 111 \rangle$ until the spots on the x-ray pictures overlapped. Then we knew that the [$\bar{1}$10] directions were lined up parallel and not antiparallel. Rotating one crystal 180° around $\langle 111 \rangle$ destroyed this overlap since $\langle 111 \rangle$ is not a twofold axis. When the spots overlapped, we knew that the absolute orientations of the two crystals were identical and that is all we needed to know to determine the relative signs of d_{14} by interference. The sign of d_{14} in GaP is also the same as in the other III-V compounds.

This result is important, because the absolute sign of d_{14} in GaP is known to be positive. This result follows from the absolute measurement of the dc electro-optic effect by Nelson and Turner[11] and the known dispersive behavior of d_{14} through the far-infrared region from the work of Faust and Henry.[12] The electro-optic coefficient is proportional to the nonlinear susceptibility given by

$$P_i{}^{\text{NLS}}(\omega) = X_{ijk}{}^{(2)}(-\omega, 0, \omega)E_j(0)E_k(\omega).$$

Since the sense of the dc electric field and the sense of the optical retardation can be determined, the electro-optic effect gives the sign of $X_{xyz}{}^{(2)}(-\omega, 0, \omega)$ directly. It was found to be positive in GaP by Nelson and Turner for frequencies ω, with photon energies below the band gap. Faust and Henry studied the nonlinear mixing given by

$$P_i{}^{\text{NLS}}(\omega_1 - \omega_2) = X_{ijk}{}^{(2)}(\omega_2 - \omega_1, -\omega_2, \omega_1)E_j(-\omega_2)E_k(\omega_1).$$

They mixed a fixed laser source at ω_1 (a He-Ne laser

[11] D. F. Nelson and E. H. Turner, J. Appl. Phys. 39, 3337 (1968).
[12] W. L. Faust and C. H. Henry, Phys. Rev. Letters 17, 1265 (1966).

TABLE III. Experimental measurements of $|d_{14}|$ (in units of 10^{-6} esu) and l_{coh} (in units of μ).

	InAs	GaAs	GaP	GaSb
$\|d_{14}\|$ (Present measurement)	1.0	0.45	0.26	$1.5_{-0.75}{}^{+1.5}$
$\|d_{14}\|$ (Patel)[a]	1.0($\pm$0.3)	0.88($\pm$0.3)	$\cdots$	$\cdots$
$\|d_{14}\|$ (Miller)[b]	$\cdots$	0.84($\pm$0.26)	0.26($\pm$0.07)	$\cdots$
$\|d_{14}\|$ (Soref and Moos)[c]	$\cdots$	0.77($\pm$0.16)	0.13($\pm$0.03)	$\cdots$
$\|d_{14}\|$ (Chang et al.)[d]	1.2($\pm$0.3)	0.9($\pm$0.2)	$\cdots$	$\cdots$
$\|d_{14}\|$ (Bloembergen et al.)[e]	$\cdots$	$\cdots$	$\cdots$	$\sim$1.0
$\|d_{14}\|$ (Nelson and Turner)[f]	$\cdots$	$\cdots$	0.105	$\cdots$
l_{coh} (Present measurement)	53($\pm$2)	104($\pm$7)	46($\pm$3)	134($\pm$7)
l_{coh} (Patel)[a]	60($\pm$10)	110($\pm$10)	$\cdots$	$\cdots$

[a] C. K. N. Patel (Ref. 2).
[b] R. C. Miller (Ref. 13). His results are converted to absolute units by taking d_{14}(KDP) $= 1.5 \times 10^{-9}$ esu $\pm 20\%$ according to R. Bechmann and S. K. Kurtz, in *Landolt-Bornstein Numerical Data and Functional Relationships*, edited by K. H. Hellwege (Springer-Verlag, Berlin, to be published), New Series, Group III, Vol. I.
[c] R. A. Soref and H. W. Moos (Ref. 14). For conversion to absolute units see Bechmann and Kurtz (Ref. b).
[d] R. K. Chang, J. Ducuing, and N. Bloembergen (Ref. 15). For conversion to absolute units see Bechmann and Kurtz (Ref. b).
[e] N. Bloembergen, R. K. Chang, J. Ducuing, and P. Lallemand (Ref. 4). For conversion to absolute units see Bechmann and Kurtz (Ref. b).
[f] See Refs. 11 and 12.

at 0.6328 μ) with a series of laser lines at ω_2 in the region of the lattice resonance. Their measurements gave the quantity $|\chi^{(2)}|^2$ as a function of frequency. By making reasonable assumptions about the form of the dispersion, they showed that $\chi_{xyz}{}^{(2)}(\omega_2-\omega_1, -\omega_2, \omega_1)$ has the same sign for $\omega_2 \to 0$ and for $\omega_2 \gg \omega_0$, where ω_0 is the lattice resonance frequency, which occurs near a wavelength of 27 μ. In the limit $\omega_2 \to 0$, we have the electro-optic effect. In the limit $\omega_2 \to \frac{1}{2}\omega_1 = \omega_L > \omega_0$, where ω_L is the CO_2 laser frequency, the susceptibility responsible for SHG is obtained:

$$\chi_{xyz}{}^{(2)}(\tfrac{1}{2}\omega_1-\omega_1, -\tfrac{1}{2}\omega_1, \omega_1) = \chi_{xyz}{}^{(2)}(-\omega_L, -\omega_L, 2\omega_L)$$
$$= \chi_{xyz}{}^{(2)}(-2\omega_L, \omega_L, \omega_L).$$

The last equality follows from the fact that $\chi^{(2)}$ is real and the cubic symmetry of the crystal.

It is thus established that the sign of d_{14} is positive in all four III-V compounds investigated, with the convention that the positive [111] direction points from a III atom to the nearest-neighbor V atom.

C. Absolute Magnitude of d_{14}

Whereas, the relative magnitudes of d_{14} from Eq. (7) are independent of the laser power and the details of its mode structure, provided they do not vary significantly as sample A is replaced by B, the absolute magnitude of d_{14} from Eq. (6) requires an absolute power measurement at both the fundamental and SH frequency. Furthermore, the pulsed output of the laser consists of about five lines with respective integrated intensities of 50, 27, 12, 8, and 3%. The power at the frequencies is not synchronous, but consists of partially overlapping pulses. Even though the spatial distribution is approximately a diffraction-limited Gaussian beam, the absolute measurement is beset by considerable uncertainties.

An Eppley thermopile was used as calibrated detector with a calibration precision of 3% claimed by the manufacturer. The time-averaged laser output power at 10.6 μ could be measured directly with the instrument, and peak powers could be estimated from the known pulse duration and repetition rate. The SH signal at 5.3 μ was too weak to be measured directly with the thermopile. Therefore, the Au-Ge detector was calibrated for cw power at 3.39 μ. The beam of a He-Ne laser at this wavelength could be measured both by this detector and the pile. The response of the Au-Ge detector to transient signal was then estimated from the known circuit constants. This involved a large uncertainty. Unfortunately the Au-Ge detector could not be calibrated directly with 10.6-μ pulses from the CO_2 laser, because it has greatly reduced sensitivity at this wavelength. A major uncertainty in the determination of $|d_{14}|^2$ from Eq. (6) comes in here. It may be as large as a factor of 3.

Next the Gaussian beam profile of the unfocused beam was measured with a variable-size aperture. The spot size of the beam focused by a BaF_2 lens with 20-cm focal length was calculated. The SHG in a thin sample which was moved through the focal region followed the predicted behavior. It is estimated that our procedure to determine $(w_1)^2$ in Eq. (6) has an uncertainty of a factor of 2.

If there were N longitudinal modes of equal strength oscillating simultaneously, a correction factor $2(1-1/N)$ should be applied to the right-hand side of Eq. (6). If the N modes, however, oscillate consecutively and do not overlap, the correction factor would be $1/N$. Since we have five partially overlapping pulses, with 50% of the integrated output in one mode, the correction factor is estimated to be about unity, with an estimated accuracy of 30%.

The measured value for the coherence length in InAs is $l_{coh} = 53 \pm 2$ μ. During the measurements, the laser peak power was 500 W. The focused spot size was $w_1 = 285$ μ. For an odd number of l_{coh}, SH peak power was $\sim 10^{-3}$ W. The InAs samples had an absorption

coefficient $\alpha_{10.6,5.3\,\mu}\sim 1$ cm^{-1}. But since maximum sample thickness was only 400 μ, absorption could be neglected. The resulting value of the nonlinear susceptibility is $d_{14}(\text{InAs})=+1.0\times10^{-6}$ esu. The claimed accuracy to within a factor of 2 is limited primarily by the uncertainty of the pulse response of the detector. Combined with the other mentioned uncertainties, this gives an uncertainty of about a factor of 4 for $(d_{14})^2$.

III. DISCUSSION OF EXPERIMENTAL RESULTS

A. Comparison with Other Experimental Data

There are several reported measurements of d_{14} in the materials we have studied. Patel[2] used a CO_2 laser to study GaAs and InAs. He employed a plane-parallel slab geometry and used the Maker experiment to measure coherence lengths. His coherence-length measurements agree with ours but his relative nonlinear susceptibility $d_{14}(\text{GaAs})/d_{14}(\text{InAs})$ differs from ours by a factor of 2. This represents a factor of 4 in power, a difference far greater than the uncertainty in the relative power measurement. Possible explanations include a difference in crystal properties due to crystal growth and preparation, or an inaccuracy resulting from free-carrier absorption in InAs. Patel had to use relatively thick samples of InAs and absorption would play an important role. Another possible explanation is that multiple reflection at the fundamental resulted in an internal fundamental field strength different from what one would estimate in the case without interference. In particular, Patel used an unfocused laser beam so there is the likelihood of overlap of the multiply reflected beams.

Except for the possible differences in the crystal properties, we avoided these pitfalls by using thin wedges. We note that several sample wedges of each crystal were prepared, but except for GaAs, only one boule of each material was available. Different wedges of the same material gave consistent results and the two different boules of GaAs also gave the same results, independent of doping and carrier concentration. In Table III we compare our results to those of Patel. We also include several other experimental measurements. These were obtained with shorter-wavelength lasers and the results are not expected to be directly comparable to ours because of dispersion. Miller's[13] results and those of Soref and Moos[14] were obtained with a 1.06-μ glass Nd^{3+} laser. For both GaAs and GaP the SH at 0.53 μ is absorbed across the band gap. The dispersion associated with this electronic resonance makes a precise quantitative comparison meaningless. But we would expect the rough order-of-magnitude

agreement that the results show. Chang et al.[15] reported on the dispersion of d_{14} in GaAs and InAs, and their results show a variation of as much as a factor of 3 in d_{14} for fundamental wavelengths between 1.06 and 0.53 μ. Table III includes their results for the fundamental at 1.06 μ. Bloembergen et al.[4] reported a value of d_{14} for GaSb at 1.06 μ in presenting the preliminary results of the investigation reported in Ref. 15. Because of lack of knowledge of the indices of refraction of GaSb in this frequency range, it was not studied in detail by Chang et al. GaSb is absorbing across the band gap for both fundamental and SH for all of the fundamental wavelengths used by Chang et al. Thus the value of $d_{14}(\text{GaSb})$ is rather uncertain.

The results of Nelson and Turner for the dc electro-optic constant in GaP in combination with the infrared dispersion data of the nonlinear susceptibility of Faust and Henry provide a value of d_{14} for frequency mixing of light, when all frequencies are in the transparent region between the lattice vibration and electronic absorption bands. In this manner Nelson and Turner found $d_{14}(\text{GaP})=+0.105\times10^{-6}$ esu for SHG in this transparent band. This is perhaps the most reliable way to determine the value of d_{14}. All other values could then be determined relative to this standard. Their value is more than a factor of 2 smaller than our absolute value.

The values of Miller and of Soref and Moos differ also by a factor of 2, with the latter being close to the Nelson-Turner result. These values refer to SHG at 0.53 μ. This wavelength falls just in the electronic absorption band, which has an edge at 0.55 μ. The nonlinearity at this frequency may therefore be expected to be somewhat larger. If we combine all these results, it is probably safer to assume that the correct value of d_{14} at 10.6 μ in InAs lies between 0.5 and 1.0×10^{-6} esu. This result is, however, not in agreement with the observed ratio of SHG in InAs and Te, and the absolute determination of d_{14} in this latter material by Patel.[1] His determination yielded $d_{11}(\text{Te})=10^{-5}$ esu, and was believed to be accurate because a phase-matched geometry could be used. Our results of a relative measurement in a phase-matched configuration gives $d_{14}(\text{Te})/d_{14}(\text{InAs})=(3.7\pm25)\%$. The uncertainty is mostly due to scatter of the data in different Te samples. The transmission through the samples varied from 35 to 43%, depending on the surface treatment. The coherence length for the light waves propagating along the y axis, with the fundamental and SH polarized along the x axis, is $l_{\text{coh}}=44\pm4$ μ. These results are in agreement with the index-of-refraction data of Caldwell and Fan.[16] Our results indicate that the nonlinear constant d_{11} in Te is at least a factor of 3 less than reported by Patel.

[13] R. C. Miller, Appl. Phys. Letters **5**, 17 (1964).
[14] R. A. Soref and H. W. Moos, J. Appl. Phys. **35**, 2152 (1964).

[15] R. K. Chang, J. Ducuing, and N. Bloembergen, Phys. Rev. Letters **15**, 415 (1965).
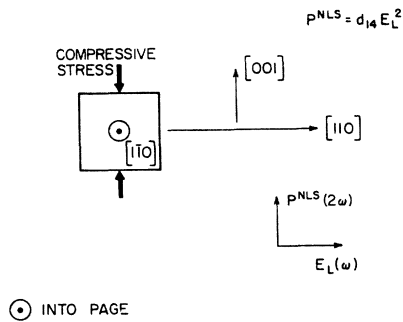[16] R. S. Caldwell and H. Y. Fan, Phys. Rev. **114**, 664 (1959).

FIG. 5. Geometry of the experiment to determine the effect of uniaxial compression on coherence length in GaAs and InAs.

B. Comparison with Theoretical Calculations

The nonlinearity d_{14} is caused by the valence electrons in the filled band and is associated with the lack of parity of the wave functions in the valence band as well as the excited bands. Although complete theoretical expressions for the nonlinear susceptibility had been given early in the development of nonlinear optics,[17-19] they are not very suitable for a numerical calculation, since they require the knowledge of the wave functions of all states in the valence band as well as the higher conduction bands.

When all frequencies involved are small compared to the electronic resonant frequencies, the linear and nonlinear susceptibilities may be expressed in terms of moments evaluated for the ground-state wave function. A localized model for the valence orbitals should yield a reasonable approximation for the macroscopic susceptibilities in the low-frequency limit.[20] The contribution of the conduction electrons in the single-band approximation vanishes because of time-reversal symmetry. The experimental and theoretical efforts of many different groups made progress simultaneously and stimulated each other. The III-V compounds with their relatively simple structure provide the first successful example of *ab initio* theoretical calculation of a nonlinear susceptibility in condensed matter. It

TABLE IV. Comparison of theoretical calculations of d_{14} to experiment (d_{14} given in units of 10^{-6} esu).

	InAs	GaAs	GaP	GaSb
Present experiment	+1.0	+0.45	+0.26	+1.51
Jha and Bloembergen (Ref. 20)	−1.5	−0.43	−0.21	−7.8
Flytzanis and Ducuing (Ref. 21)	+2.05	+0.95	+0.60	+0.80
Flytzanis (Ref. 22)	+1.1	+0.85	+0.2	+1.8
Levine (Ref. 24)	+0.96	+0.57	+0.34	+1.2
From Miller's rule[a]	1.0	0.64	0.41	1.70

[a] d_{14} calculated from Miller's rule (as given in Ref. 13): $d_{14} = \delta \chi^2(\omega)\chi(2\omega)$, where $\delta = 1.38 \times 10^{-6}$ esu is taken as constant fitted to give agreement for InAs. See also Ref. 7.

[17] P. N. Butcher and T. P. MacLean, Proc. Phys. Soc. (London) 81, 219 (1963).

[18] P. L. Kelley, J. Phys. Chem. Solids 24, 607 (1963).

[19] H. Cheng and P. B. Miller, Phys. Rev. 134, A683 (1964).

[20] S. S. Jha and N. Bloembergen, Phys. Rev. 171, 891 (1968); IEEE J. Quantum Electron. 4, 670 (1968).

is therefore appropriate to compare the experimental values with the several recent theoretical estimates.

Jha and Bloembergen[20] used linear combinations of atomic hybridized sp^3 orbitals to respresent the average ground state of the valence electrons. They used hydrogenic-type wave functions and ignored overlap. These assumptions are too crude and the calculations give the wrong sign for d_{14} as shown in the second row of Table IV. Considerably better results were obtained by Flytzanis and Ducuing,[21] who used Slater-type wave functions and a variational procedure to determine the effective charge of the bond. In particular, a higher-order variational approach in which additional parameters were adjusted gave reasonable agreement with experiment, as shown in the third row of Table IV. The local-field correction factor was chosen to yield the correct value for the linear susceptibility.

Flytzanis[22] was even more successful when he determined the expectation value of moments for the electronic-band wave function from the three-point charge model of the bond introduced by Phillips.[23] These results are shown in the fourth row of Table IV.

Levine[24] also used the Phillips bond-charge model to calculate the nonlinear susceptibilities. In his model the displacement Δr of the bond charge by an electric field is equated to the induced linear polarization. The displacement in turn produces a change in the screened Coulomb potentials from the two atoms. This change in the antisymmetric part of the crystalline potential in turn produces a change in the energy gap. This energy gap and thus the (originally linear) polarizability become field-dependent. This very simple estimate gives surprisingly good results as shown in the next to last row of Table IV. The asymmetric character of the bond is very well described by the model of electronegativity introduced by Phillips[25] and by Van Vechten.[26]

For the four compounds studied here Miller's rule is also a good guide to estimate the nonlinearity, although one should expect important deviations if the asymmetry of the charge distribution changes drastically, as discussed by Flytzanis and Ducuing.[21]

In conclusion, it may be said that reasonable quantitative agreement between theoretical calculations and observed values for the nonlinear susceptibilities has been obtained in these simple solid structures. Since Phillips's theory of electronegativity gives good results for the relationships between binding energy, linear dielectric constant, and effective band gap in a much larger variety of materials and crystal structures, it is of some interest to extend the precise measurements of the infrared nonlinear susceptibilities to other crystals.

[21] C. Flytzanis and J. Ducuing, Phys. Rev. 178, 1218 (1969).

[22] C. Flytzanis, Compt. Rend. B267, 555 (1968).

[23] J. C. Phillips, Phys. Rev. 166, 832 (1968); 168, 905 (1968).

[24] B. F. Levine, Phys. Rev. Letters 22, 787 (1969).

[25] J. C. Phillips, Phys. Rev. Letters 20, 550 (1968).

[26] J. C. Philips and J. A. Van Vechten, Phys. Rev. 183, 709 (1969).

IV. EFFECT OF UNIAXIAL STRESS ON COHERENCE LENGTH FOR SHG

Initially it was hoped that the small momentum mismatch in the far infrared of these cubic crystals could be compensated completely by a uniaxial deformation. For this purpose the change in coherence length for SHG was investigated as a function of uniaxial stress in GaAs and InAs. The geometry of the experiment is shown in Fig. 5. The 10.6-μ laser beam propagates along the $[1\bar{1}0]$ axis and is linearly polarized along the $[110]$ axis. The SH is consequently polarized along the $[001]$ axis. This is also the direction along which a compressive stress was applied by means of an hydraulic press. Two machined stainless-steel blocks were pressed against the polished (001) faces of the crystal. The stress was measured by means of a strain gauge.

The whole assembly could be turned with respect to the direction of the laser beam. The change in coherence length was determined by orientation of the crystal to a minimum (zero) in the Maker interference curve. At this setting the optical path in the crystal is an even number of coherence lengths $2M$ (where M is a large number) in length. When the stress is applied, the SH intensity goes through successive maxima and minima. Let σ_N be stress where the Nth zero is reached. At this stress the crystal is $2(M\pm N)$ coherence lengths long. The sign of the effect may be determined by starting on the slope of the Maker curve and observing whether the application of the stress causes the SH intensity to change in the same sense as the effect of an increase in optical path length l, or in the opposite sense.

It can be shown that the increase in l due to elastic distortion has an effect which is less than 1% of the photoelastic effect on the indices of refraction. In the geometry of Fig. 5, the index for the fundamental beam is changed by

$$\Delta n(\omega) = -\tfrac{1}{2}n_0^3(\omega)\pi_{12}(\omega)\sigma .$$

Here σ is the stress, which is a negative quantity for compression, and π_{12} is an element of the piezo-optical fourth-rank tensor. The index for the SH beam is changed by

$$\Delta n(2\omega) = -\tfrac{1}{2}n_0^3(2\omega)\pi_{11}(\omega)\sigma .$$

The change in the difference of the indices of the two beams by the stress σ_N is given by

$$\Delta\delta n_N = -\tfrac{1}{2}\sigma_N[\pi_{11}(2\omega)n_0^3(2\omega) - \pi_{12}(\omega)n_0^3(\omega)] . \quad (9)$$

This change is equivalent to a change in $2N$ coherence lengths of the crystal of thickness l, or

$$\Delta\delta n_N = \pm N\lambda_0/2l . \quad (10)$$

It was found that the change in index mismatch is indeed a linear function of the stress and that the slope has opposite sign for InAs and GaAs, as shown in Fig. 6. GaAs crystals have been known to withstand uniaxial
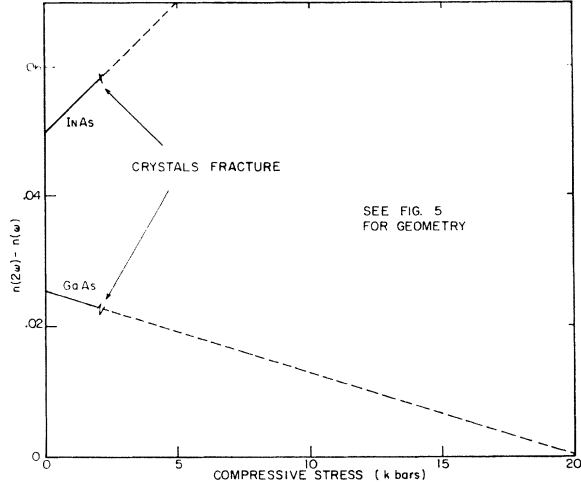

Fig. 6. Experimental results for the geometry of Fig. 5.

stresses of 10 kbar before fracturing, but in our crude apparatus fracturing occurred much sooner. Phase matching would occur at 20 kbar.

After these experiments were completed, Higginbotham et al. reported[27] a detailed study of the piezo-birefringence in GaAs as a function of wavelength from photon energies well below the band gap to energies just at the fundamental absorption edge corresponding to the direct band gap. The piezobirefringence showed negligible dispersion for photon energies below 0.4 eV and therefore their results may be meaningfully compared to ours in GaAs. Negligible dispersion means that π_{11} and π_{12} are frequency-independent between 10.6 and 5.3 μ. With the data of Higginbotham et al., one finds $1/2[\pi_{11}n_0^3(2\omega) - \pi_{12}n_0^3(\omega)] = +1.8\times10^{-3}/$ kbar, which may be compared to our value of $= +1.27$ $\times10^{-3}/$kbar from Fig. 6. (Note that σ should be taken as negative for compression.) These values differ by more than the estimated uncertainty of $\pm20\%$ in our value. In any case these two values have the same sign and are gratifyingly close in magnitude.

The results of Higginbotham et al. show that the piezobirefringence changes rapidly with frequency as the photon energy approaches the band-gap energy. In fact, the sign of the piezobirefringence changes from positive to negative for a photon energy of ~1.25 eV. The experimental results of DeMeis[28] show a strong frequency dependence of the change in the index of refraction in GaAs induced by hydrostatic pressure. If InAs is assumed to behave similar to GaAs except for a scaling of the energies in accordance with the ratio of the energy-band gaps in the two materials, we may explain the sign difference in our results for GaAs and

[27] C. W. Higginbotham, M. Cardona, and F. H. Pollak, Phys. Rev. **184**, 821 (1969).

[28] W. M. DeMeis, Harvard University Division of Engineering and Applied Physics Technical Report No. HP-15 (ARPA-16), 1965 (unpublished); Ph.D. thesis, Harvard University, 1965 (unpublished).
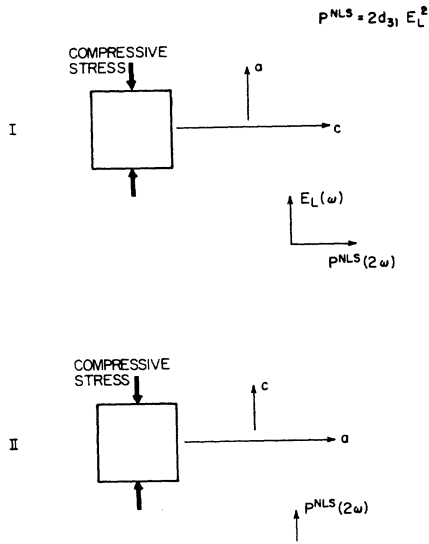
FIG. 7. Geometry of the experiment to determine the effect of uniaxial compression on coherence length in CdS and CdSe.

FIG. 8. Experimental results for the geometry of Fig. 7.

InAs. Combining the results of Higginbotham *et al.* and DeMeis, we can show that in InAs the SH photon energy is close enough to the band-gap energy to cause the sign reversal from the case of GaAs where both fundamental and SH photon energies are well below the band gap.

The GaAs data by DeMeis[28] provide a value for the quantity $\pi_{11}(\omega)+2\pi_{12}(\omega)$. His results show that this quantity is essentially frequency-independent for photon energies less than 0.5 eV. Thus it is reasonable to neglect dispersion in π_{11} and π_{12} between 5.3 and 10.6 μ, to combine our results for $\pi_{11}-\pi_{12}$ with his results for $\pi_{11}+2\pi_{12}$, and to give the resulting values of π_{11} and π_{12}. According to DeMeis, $\pi_{11}+2\pi_{12}=-13.7 \times 10^{-8}/\text{bar}$. Combined with our result, we find $\pi_{11}=-9.3\times10^{-8}/\text{bar}$ and $\pi_{12}=-2.2\times10^{-8}/\text{bar}$ for GaAs.

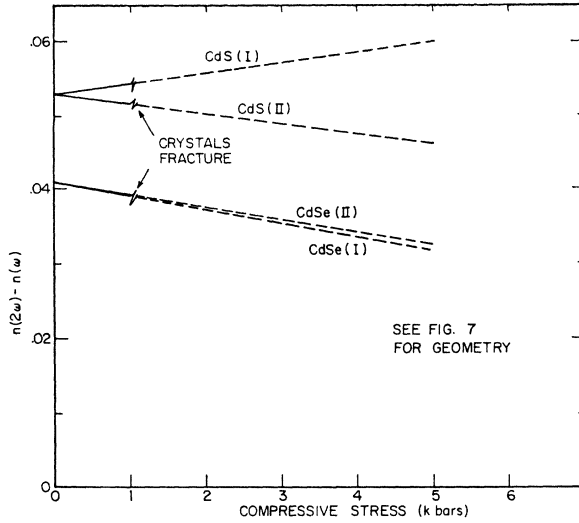Finally the results of similar experiments on two hexagonal crystals, CdS and CdSe, are presented. The

geometry of the experiment is shown in Fig. 7. In the first geometry the right-hand side of Eq. (9) must be replaced by $-\frac{1}{2}\sigma_N[\pi_{31}(2\omega)n_{c0}{}^3(2\omega)-\pi_{11}(\omega)n_{a0}{}^3(\omega)]$ and in the second geometry by $-\frac{1}{2}\sigma_N[\pi_{33}(2\omega)n_{c0}{}^3(2\omega)-\pi_{13}(\omega)n_{a0}{}^3(\omega)]$. Here the π are elements of the piezo-optic tensor is the 6*mm* point group and n_{c0} is the index of refraction for light polarized parallel to the hexagonal axis, while n_{a0} is that for light polarized perpendicular to it. The experimental results for the change of coherence length with compressive stress are shown in Fig. 8.

ACKNOWLEDGMENTS